Design of novel high-strength bainitic steels. Part II

F. G. Caballero, H. K. D. H. Bhadeshia, K. J. A. Mawella, D. G. Jones and P. Brown

Dr F. G. Caballero and Professor H. K. D. H. Bhadeshia are in the Department of Materials Science and Metallurgy, University of Cambridge, Pembroke Street, Cambridge CB2 3QZ, UK. Dr K. J. A. Mawella, D. G. Jones and Dr P. Brown are in the Structural Materials Centre, Defence Evaluation Research Agency, R1079, Bldg A7, Farnborough GU14 0LX, UK

A combination of thermodynamic, kinetic and mechanical property models and physical metallurgy principles was used in Part I of this study, to propose a number of alloys which exploit the carbide-free bainitic microstructure at its theoretical best. These alloys have been manufactured and the present paper (Part II) reports the results of metallographic characterisation and mechanical tests. The proposed steels are found to have the highest ever combination of strength and toughness for bainitic microstructures, matching even the maraging steels which are at least thirty times more expensive. The work confirms the alloy design procedures explained in Part I.

1 Introduction

A number of carbide-free bainitic steels were proposed for manufacturing in Part I of this study. The steels were designed in the basis that the fraction of bainitic ferrite obtained by continuous cooling transformation should be high enough to avoid any large and unstable regions of high-carbon retained austenite, having only the films of retained austenite to separate the bainite platelets. The steels also had to meet certain hardenability and strength requirements.

The work presented here (Part II) is concerned with the microstructural and mechanical property characterisation of the three bainitic steels proposed in Part I of this study. As will be seen later, the results are exciting.

2 Experimental procedure

The actual chemical compositions of the steels studied are given in Table 1. Alloys were prepared as 35 kg vacuum induction melts using high purity base materials. After casting and cropping, the ingots were hot forged down to a thickness of 65 mm. These were then homogenised at 1200 ^{o}C for 2 days and cut into smaller 65 mm thick samples which were then forged down to 50 mm thickness. These samples were then held at 900 ^{o}C for 2 hours, removed from the furnace and immediately hot-pressed to a thickness of 25 mm before their temperature fell below 750 ^{o}C. Finally they were allowed to cool in air. The particular deformation route used here (Fig. 1) is consistent with a proprietary manufacturing standard.

2.1 MICROSTRUCTURAL EXAMINATION OF STEELS

Quantitative X-ray analysis was used to determined the fraction of retained austenite. For this purpose, samples were cut from undeformed regions of Charpy specimens. After grinding and final polishing using 0.25 μm diamond paste, the samples were etched to obtain an undeformed surface. They were then step-scanned in a Philips - PW 1730 X-ray diffractometer using unfiltered Cu K_α radiation. The scanning speed (2θ) was 1 degree min^{-1}. The machine was operated at 40 kV and 40 mA. The retained austenite content was calculated from the integrated intensities of (200), (220) and (311) austenite peaks, and those of (002), (112) and (022) planes of ferrite.[1] Using three peaks from each phase avoids biasing the results due to any crystallographic texture in the samples.[2] The carbon concentration in the austenite was estimated by using the lattice parameters of the retained austenite.[3]

Specimens for transmission electron microscopy (TEM) were machined down to 3 mm diameter rod. The rods were sliced into 100 μm thick discs and subsequently ground down to foils of 50 μm thickness on wet 800 grit silicon carbide paper. These foils were finally electropolished at room temperature until perforation occurred, using a twin-jet electropolisher set at a voltage of 40 V. The electrolyte consisted of 5 % perchloric acid, 15 % glycerol and 80 % methanol. The foils were examined in a JEOL JEM-200 CX transmission electron microscope at an operating voltage of 200 kV.

Optical and scanning electron microscopy (SEM) were used to examine the etched microstructures. Specimens were polished in the usual way and etched in 2% Nital solution, and examined using a JEOL JXA-820 scanning electron microscope operated at 10-15 kV. The volume fraction of bainite (V_b) was estimated by a

systematic manual point-counting procedure on scanning electron micrographs.[4] A grid superimposed on the microstructure provides, after a suitable number of placements, an unbiased statistical estimate of V_b.

2.2 MECHANICAL PROPERTIES DETERMINATION

Tensile testing was carried out in accordance with BS EN 10 002-1: 1990 at room temperature on a 100 kN Instron-6025 machine at a crosshead speed of 2 mm min^{-1}. Two specimens were tested for each alloy.

Impact toughness was measured at temperatures between 20 and -120 ^{o}C using a 300 J Charpy testing machine. Specimens were tested in accordance with BS EN 10 045-1: 1990. Six specimens were tested at each temperature for every alloy.

Compact tension specimens were used to measure values of plane strain fracture toughness (K_{Ic}) at room temperature for the Ni1 and Ni2 alloys in accordance with BS 7448 Part1: 1991. Compact tension / fracture toughness testing was done on a 100 kN ESH servohydraulic machine. The crosshead speed used was 1 mm min^{-1}.

Fractography was carried on the Charpy impact toughness specimens using a JEOL JXA-820 scanning electron microscope operating at 20 kV.

2.3 TEMPERED MICROSTRUCTURES

Austenite formation begins during heating at the Ac_1 temperature and is completed when the Ac_3 temperature is reached. Tempering must be carried out below the Ac_1 temperature to avoid the accidental formation of austenite. The austenite formation temperatures were therefore determined using a Thermecmastor-Z thermomechanical

simulator. Cylindrical specimens 12 mm in height and 8 mm in diameter were heated at a rate of 10 ^{o}C s^{-1} to 1000 ^{o}C and then cooled at 10 ^{o}C s^{-1}. The Formation of austenite during heating was detected by monitoring the fractional change in dilatation with temperature. Table 2 shows the Ac_1 and Ac_3 temperatures. Note that the Ac_1 temperature is ill-defined in the present context because the microstructures already contain some retained austenite. Ac_1 should therefore be interpreted to mean the temperature at which austenite growth begins during heating at the specified rate. Specimens of the three alloys were tempered at temperatures ranging from 400 to 700 ^{o}C for an hour. Specimens for TEM were produced as described above.

3 Results and discussion

3.1 CHARACTERISATION OF MICROSTRUCTURE

Experimental data of the designed steel microstructures are presented in Table 3. These data and the micrographs presented in Fig. 2 reveal that Ni1 and Ni2 have the desired microstructure consisting of mainly bainitic ferrite and retained austenite. Because of the high carbon content in austenite (x_γ) for these alloys (Table 3), the majority of residual austenite present after bainite is formed, is retained on cooling to room temperature. In the SEM micrographs martensite regions are relatively unetched, and appear light in colour. The thin interlath films of austenite, however, have been etched away. It is difficult in thin-foil TEM experiments to judge whether any martensite has formed as a result of the thinning process or whether it was present in the original microstructure. To cope with this, the samples were tempered

at 200 ^{o}C for 2 h before making foils. Thus, martensite present in the original sample would contain carbides, whereas any untempered martensite can be interpreted to be austenite which underwent transformation during the foil preparation process. The observation of tempered microstructures (Fig. 2.*c*) showed that the unetched regions in Fig 2.*b* are martensitic. Note that the low temperature tempering (200 ^{o}C) heat treatment does not affect bainitic ferrite since the latter does not contain excess carbon.

Due to the high volume fraction of bainitic ferrite in Ni1 and Ni2 alloys, 0.62 and 0.81 respectively, the retained austenite was largely present as films between the subunits of bainitic ferrite. Figure 3 shows typical bright-field images of carbide-free upper bainite in Ni1 and Ni2 with interlath retained austenite films. These films have a typical wavy morphology characteristic of the bainite in high-silicon steels (Fig. 3.*b*).[5-8]

By contrast, the small amount of bainite in the Mn alloy (Table 3) causes much of the residual austenite to transform to martensite during cooling because of lower carbon-enrichment of the austenite (0.55 wt-%, Table 3). There is only 10 % of the residual austenite retained to room temperature (V_{γ}=0.07, Table 3). These results are consistent with the data on instability of residual austenite as function of austenite carbon content illustrated elsewhere.[9]

The results of hardness tests are presented in Table 4. There is no doubt that the microstructures of Ni1 and Ni2 alloys in the as-received condition consist mainly of bainite and retained austenite. Their hardness values are closer to those of microstructures obtained isothermally at 375 ^{o}C than the respective hardness values of the martensite as determined by water quenched following austenitisation at 1000 ^{o}C for 15 min. Any difference between the hardness values of as-received and

isothermally transformed microstructures in Ni1 and Ni2 alloys is due to the different degree of transformation to bainitic ferrite. Not surprisingly, the hardness value for the as-received microstructure of Mn alloy (Fig. 2.a) is similar to that of a fully martensitic sample.

3.2 MECHANICAL PROPERTIES

3.2.1 TENSILE STRENGTH AND DUCTILITY

Tensile test results are presented in Table 5. Plates of bainitic ferrite are typically 10 μm in length and about 0.2 μm in thickness (Fig. 3). This gives a rather small mean free path for dislocation glide. Thus, the main microstructural contribution to the strength of bainite is from the extremely fine grain size of bainitic ferrite.[10]

It is difficult to separate the effect of retained austenite on strength in these steels from other factors. Qualitatively, austenite can affect the strength in several ways. Residual austenite can transform to martensite during cooling to room temperature, thus increasing the strength as observed in Mn alloy (Tables 3 and 5). On the other hand, retained austenite interlath films can increase the strength by transforming to martensite during testing, similar to the behaviour of TRIP (transformation induced plasticity) steels.

The low yield/ultimate tensile strength ratios (YS/UTS) in Table 5 are due to the presence of austenite and the generally large dislocation density in the microstructure.[11] Consequently, retained austenite increases the strain-hardening rate of the steel. Likewise, tensile elongation is controlled by the volume fraction of retained austenite.[12] Retained austenite is a ductile phase compared to the bainitic

ferrite and would be expected to enhance ductility as far as the austenite is homogeneously distributed along plate boundaries (film austenite). However, isolated pools of austenite (blocky austenite) would influence unfavourably on both elongation and UTS. From Table 5, it is clear that the steels present a combination of high strength and good ductility. Moreover, tensile properties are much higher than those required for defence applications (Table 3 in Part I).

3.2.2 IMPACT TOUGHNESS

Charpy impact test results are listed in Table 6 for all the alloys. The levels required for defence applications in impact toughness have been also well achieved (Table 3 in Part I). A considerable improvement in toughness is obtained when the volume fraction of bainite increases in the microstructure. This improvement occurs despite the fact that the strength of the microstructures involved remains almost unchanged (Table 5). From the data in Table 3, it is evident that the volume fraction of bainite V_b and thus the carbon content of the retained austenite x_γ explains the improvement in toughness observed in Ni1 and Ni2 alloys as compared with the Mn alloy. The results are consistent with the enhancement of toughness expected when the amount of blocky austenite and martensite are reduced and, in general, when the stability of residual austenite is increased. Figure 4 shows the fracture surfaces of the Charpy impact specimens tested at room temperature. The two Ni alloys show ductile dimpled fracture surfaces whereas the Mn alloy, which contains a large amount of martensite, has many of the features of quasi-cleavage with isolated patches of ductile fracture.

3.2.3 FRACTURE TOUGHNESS

A compact tension specimen design was used with thickness B=23.1 mm, width W=46.5 mm, and crack length, a=24.5 mm, to width ratio of a/W=0.5. With the measured yield stress of 1100 MPa, this would give a plane strain, K_{Ic}, measurement capacity of ~ 300 MPa$\sqrt{m}$. In the event, none of the specimens failed at sufficiently low load to satisfy the K_{Ic} validity requirement.

The specimens showed a fairly significant non-linearity before maximum load. This disqualified the use of K_Q as a K_{Ic} measurement. The values quoted in Table 5 are for the stress intensity at maximum load, K_{max}. All the tests failed by microvoid coalescence with no sign of cleavage. Tearing was stable at maximum load under displacement control. Taking account of the non-linearity in the trace up to maximum load gives the *J*-Integral at maximum load, J_{max} and the stress intensity K_{Jmax} calculated from J_{max} values listed in Table 5.

Although the obtained fracture toughness results can not be considered valid, the results are promising in that the steels tested are so tough that larger samples would be needed to measure K_{Ic}. Toughness values of nearly 130 MPa$\sqrt{m}$ have been obtained for strength in the range of 1600-1700 MPa. The good fracture toughness obtained in these alloys is attributed to the presence of thin films of thermally and mechanically stable interlath retained austenite. The role of retained austenite is to refine the effective fracture grain size and to a blunt propagating crack.[13]

Figure 5 shows properties of mixed microstructures of bainitic ferrite and austenite, versus those of quenched and tempered (QT) low-alloy martensitic alloys and maraging steels.[7] Small points in the graph refer to previous work,[5-7,9,13] whereas the two large points correspond to experimental data shown in Table 5. The alloys

designed theoretically in this work and produced by commercial continuous cooling present the highest strength/toughness combinations ever recorded in bainitic steels. These alloys show better mechanical properties of the QT low-alloy martensitic alloys and match the critical properties of maraging steels, which are at least thirty times more expensive.

3.3 CHARACTERISATION OF TEMPERED MICROSTRUCTURES

Figure 6 shows a plot of hardness values as a function of tempering temperature for the three studied alloys. Tempering the designed microstructures of Ni1 and Ni2 steels at temperatures lower than 550 ^{o}C for an hour did not result in any significant loss of hardness. However, tempering at 450 ^{o}C for an hour the as-received microstructure of Mn alloy led to a drop in the hardness value from 597 to 555 HV. Since the Mn alloy contains predominantly martensite ($V_{\alpha'}$ = 0.67, Table 3) tempering at 400 ^{o}C for an hour is expected to lead to the precipitation of any excess carbon. This is confirmed by Fig. 7.a which shows discrete carbide particles precipitated inside a martensite plate in the Mn alloy. The retained austenite was still intact with no significant signs of recovery in the bainitic ferrite.

Figures 7.b and c show bright-field images of microstructures obtained by tempering at 400 ^{o}C for an hour in Ni1 and Ni2 alloys. Comparing tempering microstructures with those as-received conditions (Fig. 3), it is clear that the tempering at 400 ^{o}C did not result in any recovery in the bainitic ferrite (Fig. 7.b) or in the diffusional decomposition of high carbon retained austenite (Fig. 7.c and d).

4 Conclusions

It has been demonstrated experimentally that models based on phase transformation theory can be applied successfully to the design of high strength and tough steels. These alloys designed to ensure that the hardenability of the steel is sufficient for industrial production have achieved the highest strength and toughness combinations to date for bainitic steels, at a cost thirty times less than that of maraging steels. Likewise, it has been found that these two new steels also show an important resistant to tempering. Steels have been tempered at temperatures ranging from 400 to 700 ^{o}C for an hour and no significant changes in hardness were detected in the microstructure at tempering temperatures lower than 550 ^{o}C.

5 Acknowledgments

This work was carried out as part of Technology Group 4 (Materials and Structures) of the MoD Corporate Research Programme. The authors would like to thank to Professor Alan Windle for the provision of laboratory facilities at the University of Cambridge.

6 References

1. J. DURNIN and K. A. RIDAL: *Journal of the Iron and Steel Institute,* 1968, **206**, 60.
2. M. J. DICKSON: *J. Appl. Cryst*., 1969, **2**, 176-180.
3. D. J. DYSON and B. HOLMES: *Journal of the Iron and Steel Institute,* 1970, **208,** 469.
4. G. F. VANDER VOORT: 'Metallography. Principles and Practice', 427; 1984, New York, McGraw-Hill.
5. V. T. T. MIIHKINEN and D. V. EDMONDS: *Mater. Sci. Technol*., 1987, **3**, 422-431.
6. V. T. T. MIIHKINEN and D. V. EDMONDS: *Mater. Sci. Technol*., 1987, **3**, 432-440.
7. V. T. T. MIIHKINEN and D. V. EDMONDS: *Mater. Sci. Technol*., 1987, **3**, 441-449.
8. L. C. CHANG: *Metall. Trans*., 1999, 30A, 909-916.
9. H. K. D. H. BHADESHIA and D. V. EDMONDS: *Metal Sci.,* 1983, **17**, , 411-419.
10. K. J. IRVINE, F. B. PICKERING, W. C. HESELWOOD and M. J. ATKINS: *J. iron Steel Inst.*, 1957, **195**, 54-67.
11. A. P. COLDREN, R. L. CRYDERMAN and M. SEMCHYSHEN: 'Steel Strengthening Mechanisms', 17; 1969, Ann Arbor, USA, Climax Molybdenum.
12. B. P. J. SANDVIK and H. P. NEVALAINEN: *Met. Tech*., 1981, **15**, 213-220.
13. H. K. D. H. BHADESHIA and D. V. EDMONDS: *Metal Sci*., 1983, **17**, 420-425.

Table 1 Actual Chemical Composition of Designed Alloys, wt-%

Alloy	C	Si	Mn	Ni	Cr	Mo	V
Mn	0.32	1.45	1.97	<0.02	1.26	0.26	0.10
Ni1	0.31	1.51	<0.01	3.52	1.44	0.25	0.10
Ni2	0.30	1.51	<0.01	3.53	1.42	0.25	<0.005

Table 2 Ac_1 **and** Ac_3 **Temperatures in** ^{o}**C**

Alloy	Ac_1	Ac_3
Mn	807	881
Ni1	759	818
Ni2	775	835

Table 3 Quantitative Data on Microstructure and Hardness*

Alloy	V_b	V_γ	$V_{\alpha'}$	x_γ, wt-%	Hardness, HV30
Mn	0.26±0.01	0.07±0.01	0.67±0.02	0.55	597±2
Ni1	0.62±0.05	0.12±0.01	0.26±0.04	0.92	493±5
Ni2	0.81±0.06	0.11±0.01	0.08±0.05	1.03	536±6

V_b bainitic ferrite volume fraction; V_γ retained austenite volume fraction; $V_{\alpha'}$ martensite volume fraction; x_γ carbon content in austenite

*Hardness values are averaged over 10 tests

Table 4 Hardness Data of Different Microstructures of the Alloys Studied

Alloy	Heat treatment	Hardness, HV30*
Mn	As received microstructure	597±2
	WQ†	605±5
	350 ^{o}C for 30 min, WQ	467±7
Ni1	As received microstructure	493±5
	WQ	647±8
	375 ^{o}C for 30 min, WQ	426±4
Ni2	As received microstructure	536±6
	WQ	669±7
	375 ^{o}C for 30 min, WQ	423±9

*Hardness values are averaged over 10 tests

†WQ water quench

Table 5 Tensile* and Fracture Toughness† Properties

Alloy	YS MPa	UTS MPa	Elongation %	RA %	K_{max} MPa$\sqrt{m}$	J_{max} MPa m	K_{Jmax} MPa$\sqrt{m}$
Mn	1167	1790	13	44			
Ni1	1150	1725	14	55	125	0.114	160
Ni2	1100	1625	14	59	128	0.134	174

*YS yield strength; UTS ultimate tensile strength; RA reduction of area.

†K_{max} stress intensity factor at maximum load; J_{max} J-integral at maximum load; K_{Jmax} stress intensity values calculated from J_{max} values.

Table 6 Charpy Impact Test Results*

Alloy	Test temperature, ^{o}C	Impact energy, J
Mn	20	34±1
	-40	31±1
Ni1	20	58±2
	-40	46±1
	-120	34±2
Ni2	20	50±3
	-40	43±1
	-120	25±3

*Each value is a mean of six tests

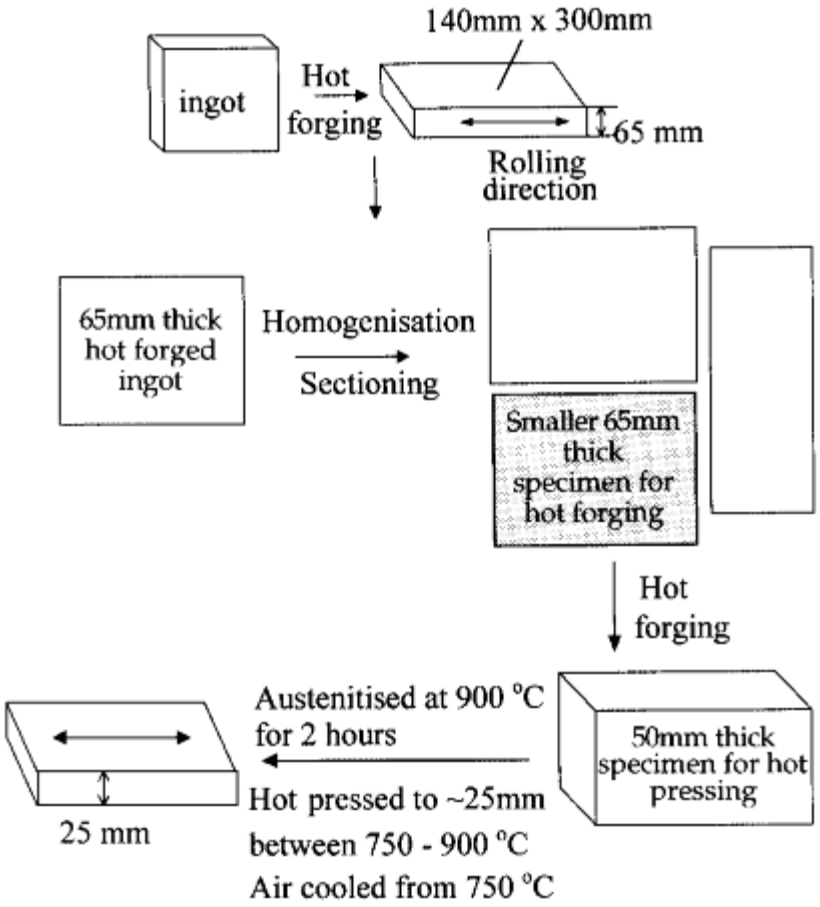

Figure 1 Manufacturing route

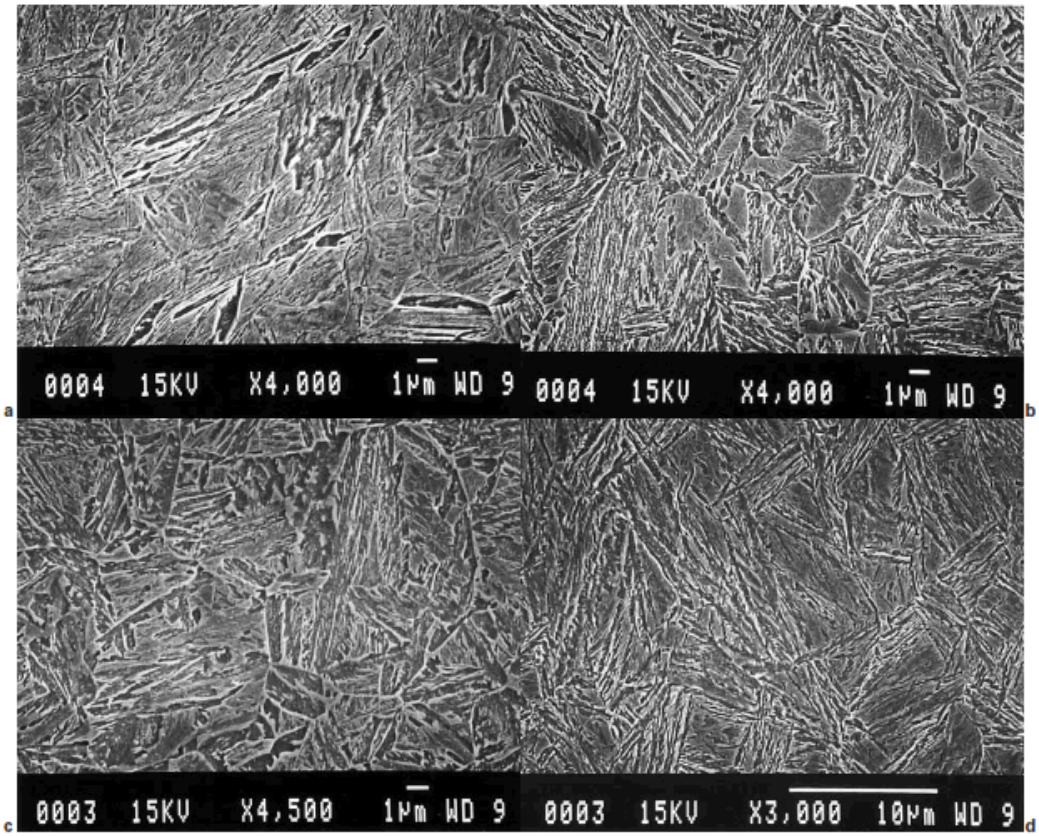

a Mn alloy as received microstructure; *b* Ni1 alloy as received microstructure; *c* Ni1 alloy as tempering at 200 ^{o}C for 2 hrs. microstructure; *d* Ni2 alloy as received microstructure

Figure 2 Scanning electron micrographs of microstructures in the designed alloys

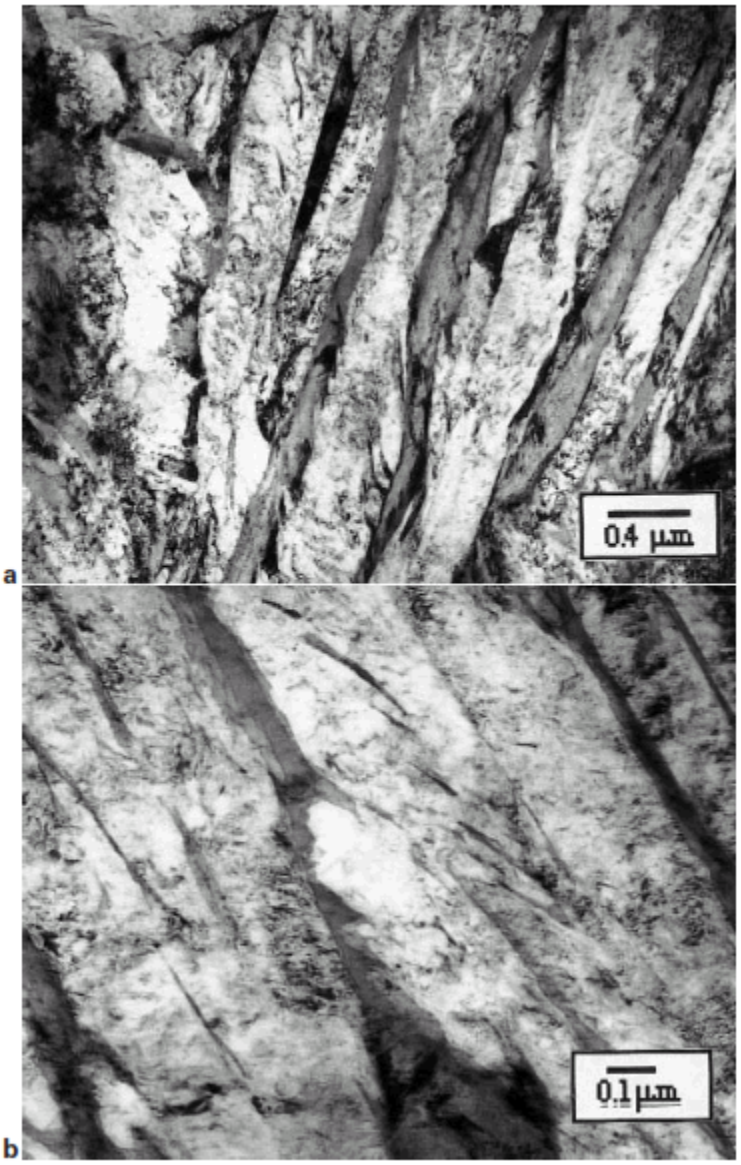

a Ni1 alloy; *b* Ni2 alloy

3 Typical bright field images of microstructures formed by bainitic ferrite and films of retained austenite

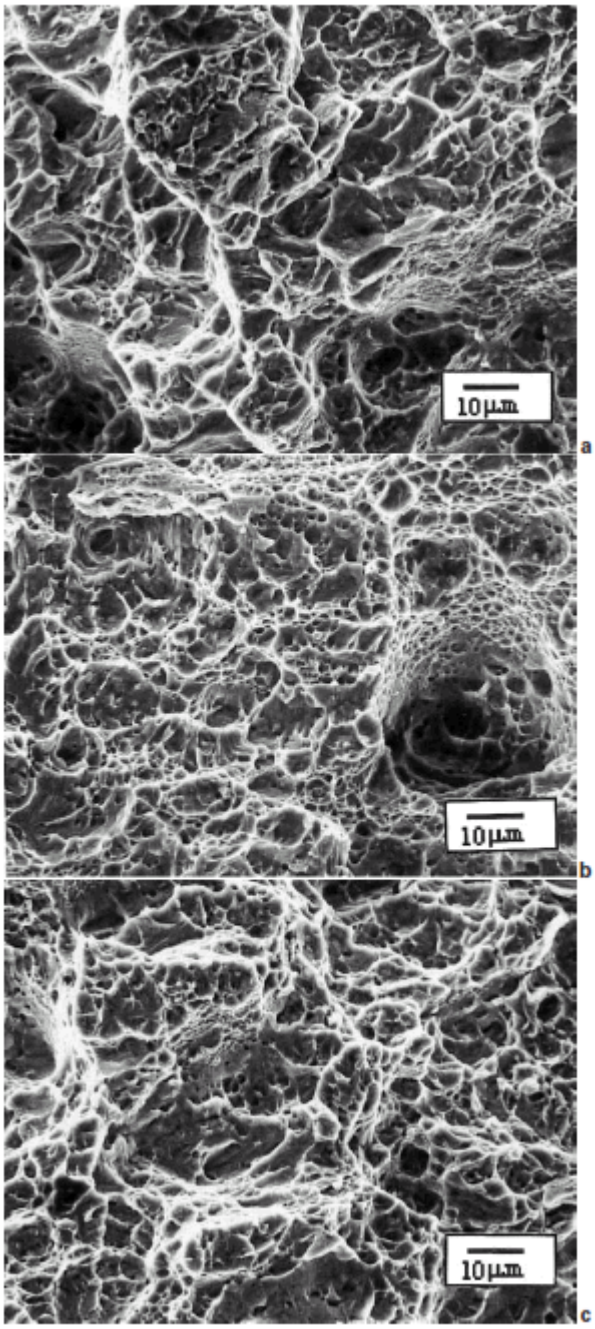

a Mn alloy, room temperature; *b* Ni1 alloy, room temperature; *c* Ni2 alloy, room temperature

4 Fracture surfaces of Charpy impact specimens tested at different temperatures. Scanning electron micrographs

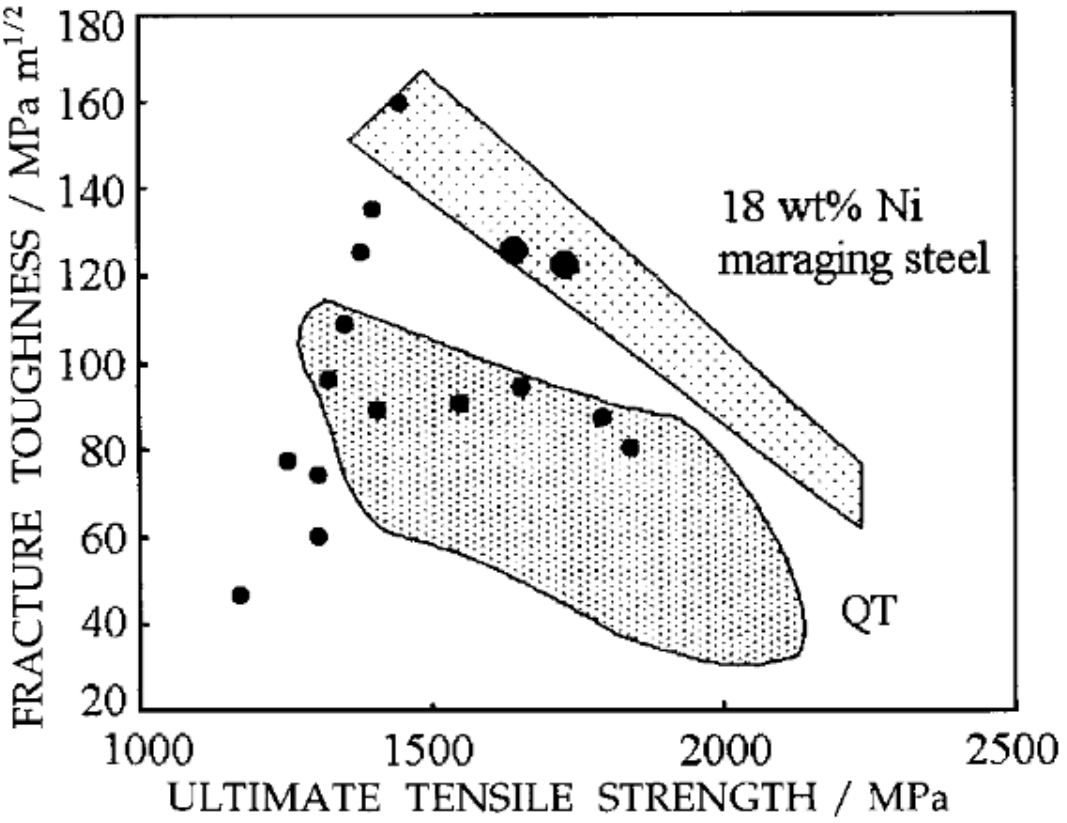

5 Properties of mixed microstructures of bainitic ferrite and austenite, versus those of quenched and tempered (QT) low-alloy martensitic alloys and maraging steels

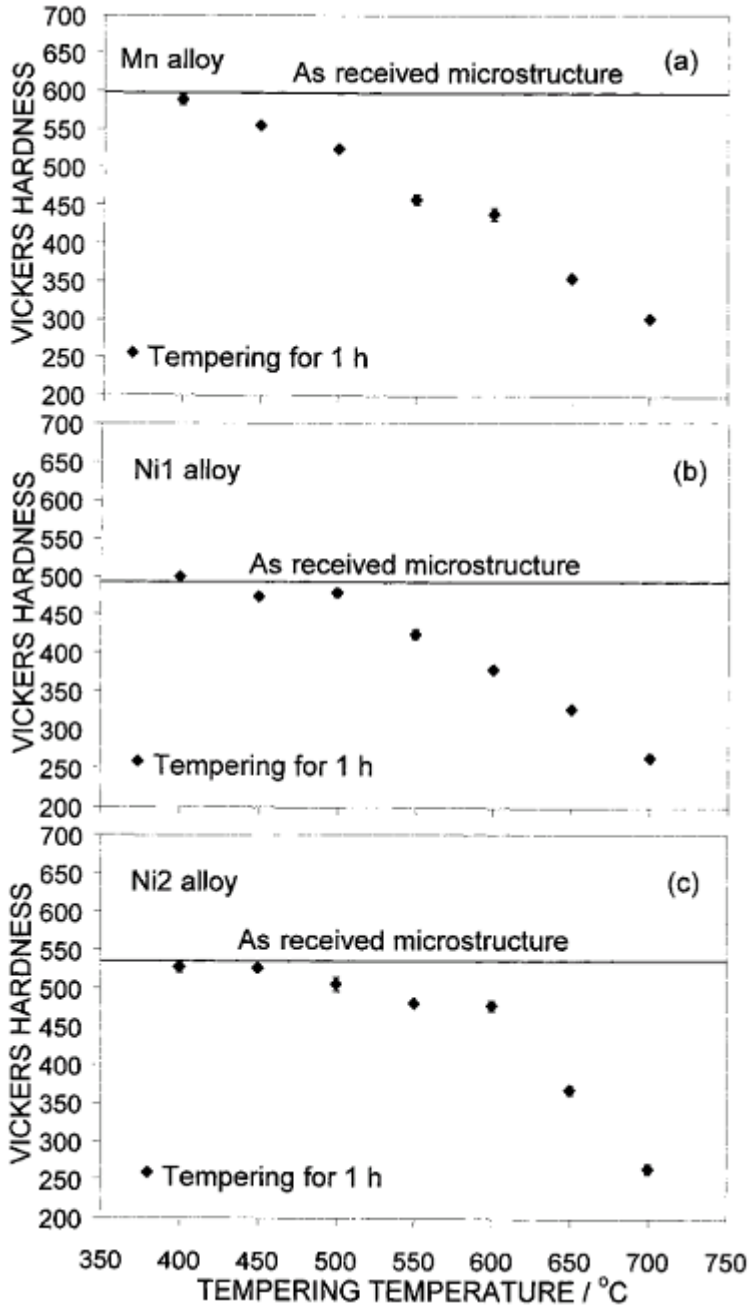

a Mn alloy; *b* Ni1 alloy; *c* Ni2 alloy

6 Plot of hardness values as a function of tempering temperature

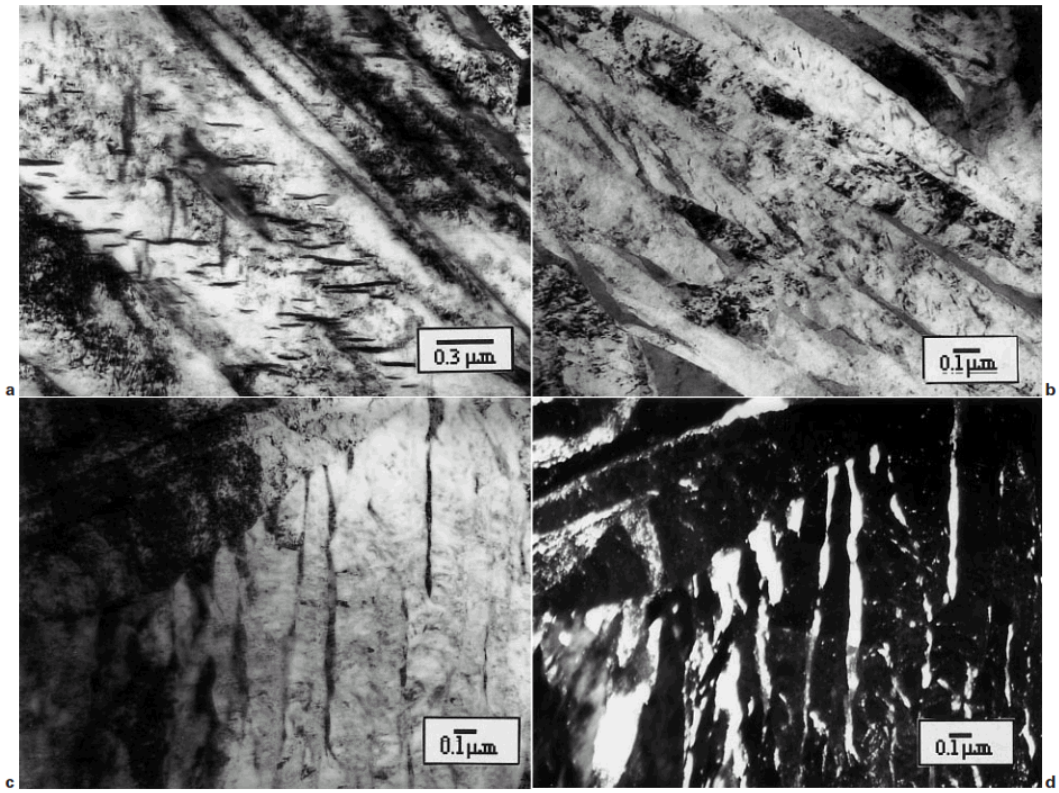

a Discrete carbide particles precipitate inside a martensite plate in Mn alloy; *b* None sings of recovery occur in the bainitic microstructure of Ni1 alloy; *c* Bright field and *d* dark field images reveal that retained austenite is still intact in Ni2 alloy

7 Transmission electron micrographs of microstructures obtained by tempering at 400 ^{o}C for an hour